ΔN interaction and πd observables

Sarah C. B. Andrade and Erasmo Ferreira
Departamento de Fisica, Pontificia Universidade Catolica, Rio de Janeiro 22452, Brasil

H. G. Dosch
Institut für Theoretische Physik der Universität, D-6900 Heidelberg, Federal Republic of Germany
(Received 15 July 1985)

With the double purpose of improving the theoretical description of πd observables and of obtaining information on the ΔN interaction parameters, we add to sets of amplitudes obtained from three-body calculations of πd scattering the contributions due to the short range ΔN interaction in the intermediate state. The full amplitudes are used to fit the experimental data on differential cross section and vector analyzing power at 142, 180, and 256 MeV pion kinetic energies, while the free ΔN parameters are determined, with attention given to possible resonant forms in the $J^P=2^+$, 3^-, and 4^+ states. Our results, for two independent sets of three-body amplitudes, show that the ΔN interaction in the $^5S_2$ and $^5P_3$ waves give very important additional contributions, with remarkable improvement in the description of the data. However, in the limited conditions of our experimentation, we cannot prove the existence of a clean resonant character in these interactions. The contributions of other ΔN low orbital angular momentum waves, such as $^3S_1$ and $^5D_4$, give additional improvements to the fittings, but we must be aware that quantitative conclusions about the corresponding ΔN parameters may be affected by uncertainties in the background amplitudes.

I. INTRODUCTION

The measurements of polarization observables in πd reactions and the question of the possible existence of dibaryonic states have reinforced the need for more complete and more reliable theoretical calculations of πd amplitudes. Although Faddeev calculations of πd scattering[1-3] give in general a reasonable description of the differential cross section, except for the well-known deviations in the region of large momentum transfers, they are not consistent with each other in the individual amplitudes, and consequently in the values predicted for the vector polarization and other observables. On the other hand, the importance of the Δ excitation and of the ΔN dynamics (which are expected to play a fundamental role in the formation of dibaryonic states) is not fully accounted for in the conventional three-body Faddeev calculations.

The investigation of nonstandard contributions, like the formation of exotic six-quark states as intermediate contributions to πd scattering, can only be made using as background a reliable set of conventional theoretical amplitudes, which should include all ΔN dynamics, besides the NN and Nπ interactions used in the description of the three-body NNπ system. The description of the Δ as a composed Nπ system while moving inside the nuclear matter (even in the deuteron) is not necessarily realistic and may not account for important contributions. The fully consistent inclusion of the Δ particle in the theoretical calculation would lead us to a four-body problem, which is not yet accessible to a practical treatment. A first approximation towards the treatment of this problem consists in adding to the Faddeev amplitudes the contributions of the diagram of Fig. 1, which represents the effects of the ΔN interaction in the intermediate state of πd elastic scattering. We must remark that, in order to avoid double counting, these added contributions can only refer to terms which cannot be reduced to a succession of NN and Nπ scatterings and thus contain mainly the short range ΔN contributions, including possible effects due to dibaryon formation. It is important to note that the diagram of Fig. 1 only accounts for conventional states of baryon number 2, i.e., states formed of two strongly interacting distinct baryons.

Unfortunately we do not know enough about the ΔN system to make a quantitative evaluation of the above mentioned terms. The studies of the coupled channel NN, NΔ, and ΔΔ systems[4] have not yet been able to give unique information on the ΔN parameters. We can then invert the problem, and use the πd system as a laboratory to extract information on the ΔN system. In previous papers[5-7] we have obtained expressions for the contributions to the πd helicity amplitudes due to the diagram of Fig. 1. We have evaluated[7] form factors $F_L(s)$ which represent contributions due to the ΔN interaction in a relative orbital angular momentum L, and have shown that $F_L(s)$ de-

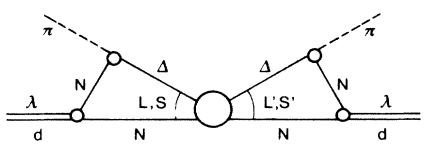

FIG. 1. Skeleton diagram representing contributions due to the ΔN→ΔN interaction in the intermediate state of πd elastic scattering. L and S represent the relative orbital momentum and the total spin, respectively, of the ΔN system.

TABLE I. Angular momentum and spin states used in the present work for the investigation of the ΔN interaction. Only the waves with lowest possible L values for each J and parity quantum numbers are considered.

J^P	L	S
0^+	2	2
1^+	0	1
1^-	1	1
1^-	1	2
2^+	0	2
2^-	1	1
2^-	1	2
3^-	1	2
4^+	2	2

creases sharply with increasing values of L, so that the strongest contributions to the diagram are expected to come from the lowest L values.

The purpose of the present work is to use the ΔN interaction to fill up discrepancies between the theoretical and the experimental values for the πd observables of differential cross section and vector analyzing power iT_{11}. We treat the ΔN interaction in the zero width approximation for the Δ, i.e., we treat the Δ as an elementary hadron. This is consistent with the interpretation of the Δ as a genuine three-quark state. In the propagator for the evaluation of the vertex function the finite width has been taken into account as explained in Ref. 6. We describe the ΔN interaction in each partial wave listed in Table I through a set of free parameters (phase shifts and absorption coefficients), which are determined through a best fitting procedure. We search simultaneously for the contributions of resonant dibaryonic interactions in the states shown in Table II, and determine the strengths of the relevant couplings. However, our calculation of additional contributions to the πd amplitudes is not committed to the existence of these dibaryonic states.

In our dynamical scheme, dibaryons may couple to the ΔN and NN systems, not directly to πd. The unitarity restrictions which constrain our evaluation of the diagram represented in Fig. 1, as explained in detail in Refs. 5–7, and the energy dependence of the evaluated contributions (largely determined by the vertex functions representing the triangular structures) are characteristic of the dynamical model adopted here. This is in contrast with the investigations where elementary π-d dibaryon couplings have been assumed.[8]

In the present work we make use of two independent sets of three-body πd amplitudes, which we identify,

TABLE II. Possible dibaryon resonances which have been included in our investigation of the ΔN interaction.

J^P	Mass m_B (GeV)	Width Γ_B (GeV)	L
2^+	2.15	0.10	0,2,4
3^-	2.23	0.14	1,3,5
4^+	2.48	0.15	2,4,6

respectively, as RS (from Rinat-Starkand[1]) and Lyon[2] amplitudes. In Sec. II we present the formulae for the corrections to the πd helicity amplitudes due to the ΔN interaction in the intermediate state, according to the dynamical model of Fig. 1. In Sec. III we present the results of the fittings to the experimental data on the observables of differential cross section and vector analyzing power. We work at the pion kinetic energies of 142, 180, and 256 MeV, which cover the relevant range, and where data[9–12] and background amplitudes are available. We do not include the tensor polarization t_{20} in the fitting, due to the present ambiguities in the experimental data. Instead, from the fittings of $d\sigma/d\Omega$ and iT_{11}, we evaluate the expected values for t_{20}. Finally, in Sec. IV we summarize and discuss the results obtained.

II. CONTRIBUTIONS TO THE πd AMPLITUDES

We evaluate the full scattering amplitude as a sum of the background amplitudes derived from a three-body Faddeev calculation plus the contributions from the diagram represented in Fig. 1. The form of these contributions has been derived in Ref. 6 for the $J^P=2^+$, $L=0$, $S=2$ state (L is the relative orbital angular momentum and S the total spin of the ΔN system), with a detailed treatment of the deuteron wave function. The vertex functions corresponding to ΔN interaction in states of arbitrary orbital angular momentum have been obtained[7] neglecting the small d wave component in the deuteron wave function and somewhat simplifying the Fermi motion corrections in the evaluation of the triangular diagrams. These simplifications were seen to introduce modifications of the order of only a few percent in the amplitudes, and allowed us to obtain very transparent expressions for the vertex functions representing the dynamical structure.

We now write the expressions for the contributions of the ΔN interaction to the πd helicity amplitudes, in the general case. For transition from initial λ to final λ′ helicities, the form for these contributions is

$$f_{\lambda'\lambda}(\theta)=\sum_J \frac{16}{9\pi\sqrt{s}} g^2_{\Delta N\pi} |\mathbf{q}_\pi|^2 \sum_{LSL'S'} [F_L(s)K^{(S)}\langle SL;\lambda 0|J\lambda\rangle\langle 1,1;\lambda 0|S\lambda\rangle \times F_{L'}(s)K^{(S')}\langle S'L';\lambda' 0|J\lambda'\rangle\langle 1,1;\lambda' 0|S'\lambda'\rangle \mathcal{M}^{SL;S'L';J}_{\Delta N\to\Delta N}(s)] d^J_{\lambda'\lambda}(\theta) . \quad (1)$$

This form generalizes Eqs. (5) and (6) of Ref. 6. The definition of the vertex functions $F_L(s)$ is presented in Ref. 7, where their numerical values are also given, for the energies of interest for the present work. For the case $L=0$, the vertex function $F_L(s)$ coincides with $M^{\Delta,1}(s)$ of Ref. 6, except for the above mentioned simplifications in the calculation.

The coefficients $K^{(S)}$ for the two possible spin states are

$$K^{(S)}=\begin{cases}\dfrac{1}{\sqrt{3}} & \text{for } S=1\\ 1 & \text{for } S=2\end{cases} . \tag{2}$$

$\mathbf{q}_\pi$ represents the pion momentum in the πd center of mass frame, and s is the usual Mandelstam variable. For the $\Delta N\pi$ coupling constant we use $g^2_{\Delta N\pi}/4\pi=20.4$ GeV^{-2}.

For the $\Delta N\to\Delta N$ amplitudes we use either general forms defined through phase shifts and inelasticity parameters, or Breit-Wigner resonance forms. Thus, for a transition between two ΔN states of the same L,S values, we write

$$\mathcal{M}^{SL;SL;J}_{\Delta N\to\Delta N}(s)=\frac{\pi}{m_N m_\Delta}\frac{\sqrt{s}}{2\mathrm{Re}(\mathbf{q}_\Delta)}T^J_{L,L;S,S}(s) \tag{3}$$

where

$$T^J_{L,L;S,S}(s)=\frac{1}{2i}(\eta^J_{L,S}e^{2i\delta^J_{L,S}}-1) . \tag{4}$$

For a resonant interaction with central mass m_B and width Γ_B we write instead

$$\mathcal{M}^{SL;S'L';J}_{\Delta N\to\Delta N}(s)=\frac{\pi}{m_N m_\Delta}g^{J,L',S'}\times\frac{1}{(m_B^2-s)-i\Gamma_B m_B}g^{J,L,S} . \tag{5}$$

The coupling constants $g^{J,L,S}$ of the ΔN system to the dibaryon states are parametrized in the form

$$\begin{aligned} g^{J,L=J-2,S=2}&=g_J\cos E_J\cos H_J ,\\ g^{J,L=J,S=2}&=g_J\sin E_J\cos F_J\cos H_J ,\\ g^{J,L=J+2,S=2}&=g_J\sin E_J\sin F_J\cos H_J ,\\ g^{J,L=J,S=1}&=g_J\sin H_J .\end{aligned} \tag{6}$$

In the transition amplitudes defined by Eqs. (3) and (4) no assumption is made of a resonantlike energy dependence in the ΔN interaction. Transitions between states with different values of L (and same J) do not occur for the selected set of states in Table I. Transitions between states with $S=2$ and $S=1$ may occur, but our numerical work has shown that the possible cases (see the 1^- and 2^- states in Table I) are not at all relevant. Therefore, to avoid unnecessary formal complications, we have written Eq. (3) without including such transition terms.

In Eq. (3) the Δ momentum in the center of mass frame $\mathbf{q}_\Delta$ is evaluated through

$$\mathbf{q}_\Delta=\frac{1}{2\sqrt{s}}[(s+m_\Delta^2-m_N^2)^2-4sm_\Delta^2]^{1/2} \tag{7}$$

with complex Δ mass $m_\Delta-(i/2)\Gamma_\Delta$. Numerically, we use $m_\Delta=1.211$ GeV and $\Gamma_\Delta=0.1$ GeV.

The fitting procedure searches for the best values of g_J, E_J, F_J, and H_J for each resonance, and for the phase shifts $\delta_{J,L,S}$ and absorption coefficients $\eta_{J,L,S}$ for each of the states listed in Table I.

The full helicity amplitudes, determined by the sum of the background Faddeev amplitudes with the contributions evaluated through Eq. (1), are taken into the expressions for the fitted observables, which are the differential cross section

$$\frac{d\sigma}{d\Omega}=\tfrac{1}{3}\sum_{\lambda,\lambda'}|f_{\lambda'\lambda}|^2 \tag{8}$$

and the vector analyzing power

$$iT_{11}(\theta)=-\sqrt{6}\,\mathrm{Im}[f^*_{10}(f_{11}-f_{1-1}+f_{00})]/(3\,d\sigma/d\Omega) . \tag{9}$$

Once the ΔN parameters are chosen, we evaluate the components of the tensor polarization in the c.m. system

$$t_{20}(\theta)=\sqrt{2}(|f_{11}|^2+|f_{1-1}|^2-|f_{10}|^2-|f_{00}|^2)/(3\,d\sigma/d\Omega) , \tag{10}$$

$$t_{21}(\theta)=\sqrt{6}\,\mathrm{Re}[f^*_{10}(-f_{11}+f_{1-1}+f_{00})]/(3\,d\sigma/d\Omega) , \tag{11}$$

and

$$t_{22}(\theta)=\sqrt{3}[2\,\mathrm{Re}(f_{11}f^*_{1-1})-|f_{10}|^2]/(3\,d\sigma/d\Omega) . \tag{12}$$

The experimentally observed values of the tensor polarization t^{lab}_{20} are determined through

$$t^{\mathrm{lab}}_{20}(\theta)=\tfrac{1}{2}(3\cos^2\beta-1)t_{20}-\sqrt{3/2}\sin(2\beta)t_{21}+\sqrt{3/2}\sin^2\beta t_{22} , \tag{13}$$

where β is the angle given by

$$\beta=\theta^{\mathrm{d}}_{\mathrm{c.m.}}-\theta^{\mathrm{d}}_{\mathrm{lab}}=\pi-\theta-\theta^{\mathrm{d}}_{\mathrm{lab}} \tag{14}$$

with

$$\tan\theta^{\mathrm{d}}_{\mathrm{lab}}=2m_{\mathrm{d}}\sqrt{s}\,\sin\theta/[(1-\cos\theta)(s+m^2_{\mathrm{d}}-m^2_\pi)] . \tag{15}$$

For $\theta=0$, one takes $\theta^{\mathrm{d}}_{\mathrm{lab}}=\pi/2$.

III. RESULTS

The sets of πd amplitudes obtained by Rinat and Starkand[1] (here called RS amplitudes) and by the Lyon group[2] were used separately as backgrounds to test the effects of the ΔN interaction in the intermediate state. We have experimented with all ΔN states shown in Table I and II.

We have considered two principal cases:

(1) First we took only into account the contribution of the conjectured dibaryon states with spin and parity $J^P=2^+$, 3^-, and 4^+ (see Table II). These states may couple to the ΔN system in orbital angular momentum $L=J-2$, J, $L+2$ and total spin $S=1$ or 2.

(2) Secondly, we took the ΔN interaction of the general form of Eq. (3) with unconstrained energy dependence of the phase shifts δ and absorption parameters η. In that case we took only into account the contribution of states with the lowest possible L value for a given J, since according to our previous analysis[7] these values of L give by far the most important contributions. We have also considered, in addition to these low L partial waves with unconstrained energy dependence, the contributions of possi-

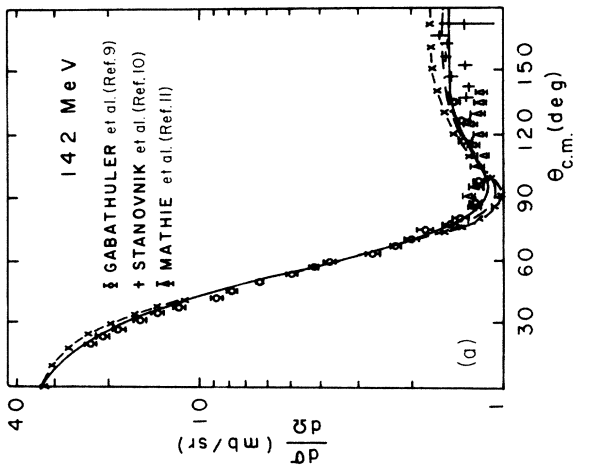

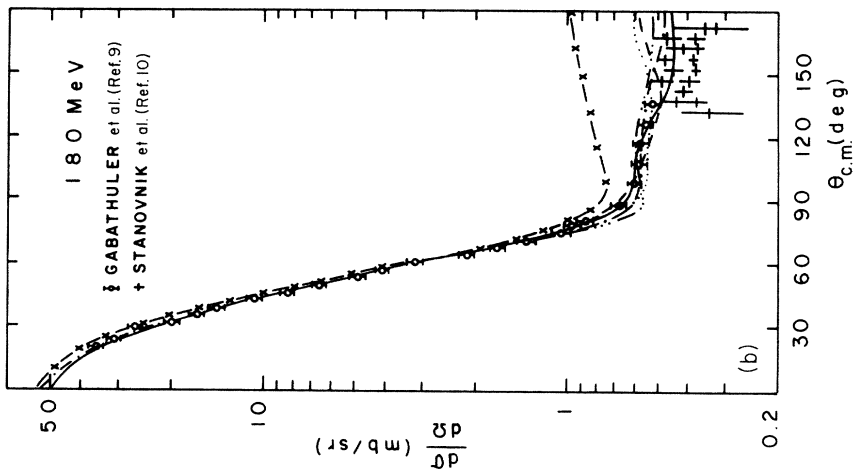

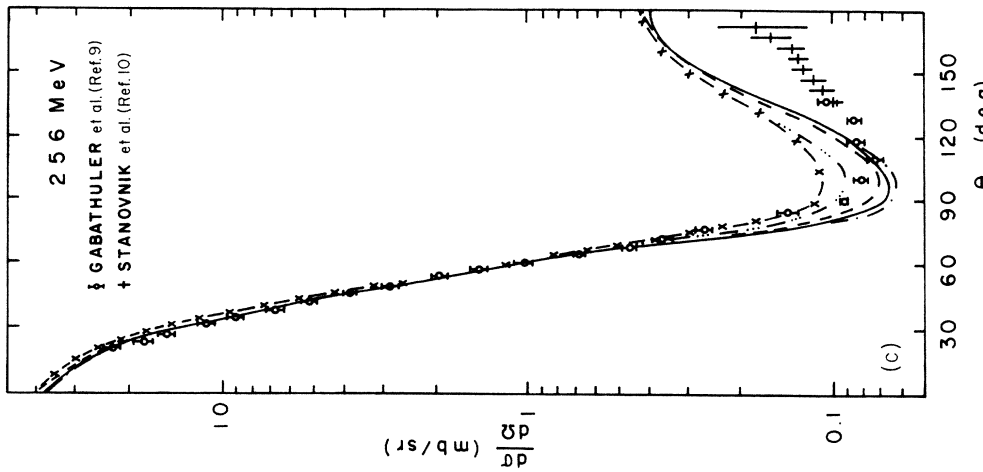

FIG. 2. (a)—(c) πd differential cross section at three values of pion laboratory energy. The dash-cross curves correspond to the Faddeev calculations of Rinat-Starkand (RS). The other curves result from simultaneous fittings of the vector analyzing power iT_{11} and the differential cross section $d\sigma/d\Omega$ at the same energies (142, 180, and 256 MeV), with the contributions of the ΔN interaction added to the RS amplitudes: (i) full line, 1^+ ($L=0$), 2^+ ($L=0$), 3^- ($L=1$) waves plus $J^P=2^+,3^-$ dibaryon resonances; (ii) dashed line, 1^+ ($L=0$), 2^+ ($L=0$), 3^- ($L=1$) waves; (iii) dot-dashed line 2^+ ($L=0$), 3^- ($L=1$) waves plus $2^+,3^-$ resonances; (iv) dotted line, 2^+ ($L=0$), 3^- ($L=1$) waves; (v) three dot-dashed line, $2^+,3^-$ resonances. Some curves are omitted due to superposition with others. The contribution of pure resonances (v) is significant only at 180 MeV, giving a very slight improvement at 256 MeV. In (a), cases (v) (three dot-dashed), (iv) (dotted), and (ii) (dashed) coincide, respectively, with the dash-cross RS background, (iii) (dot-dashed) and (i) (full). In (c) case (iv) (dotted) is superposed with case (iii) (dot-dashed).

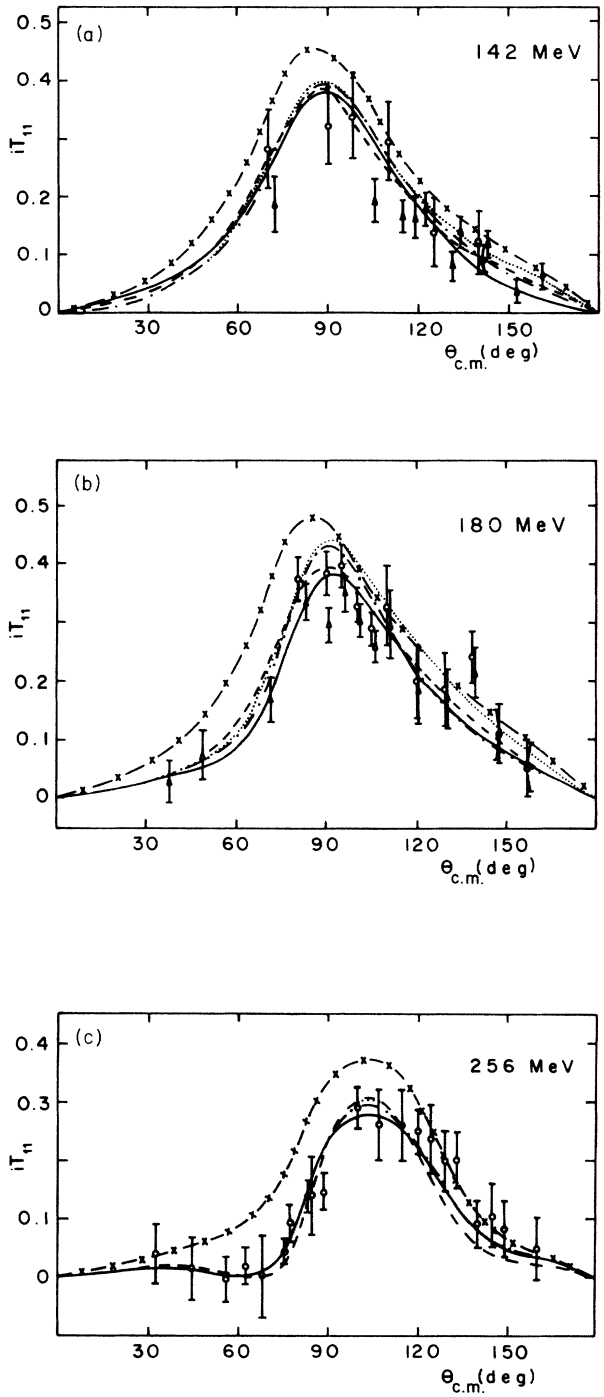

FIG. 3. (a)–(c) Vector analyzing power iT_{11} at three values of pion laboratory energy, evaluated with background of RS amplitudes plus contributions from the ΔN interaction. For meaning of curves see caption to Fig. 2. The experimental points are from Smith *et al.* (Ref. 12). In (a) the dotted and the dot-dashed lines coincide for small angles and between 90 and 120 degrees. In (c) the dotted and dot-dashed curves are distinct, respectively, from the dashed and the full lines only in the region about 100 degrees. The pure resonance case (corresponding to the three dot-dashed line in Fig. 2) results are worse than the pure background at all energies, and the corresponding curves are not drawn.

bly resonant higher partial orbitals.

We found it very important to fit simultaneously the experimental data for $d\sigma/d\Omega$ and $iT_{11}(\theta)$, since a fit of iT_{11} alone may lead to very bad results for the differential cross section.

The fitting of the experimental data was made with the CERN MINUIT program, searching for values of the phases $\delta_{J,L,S}$, the absorption coefficients $\eta_{J,L,S}$, and the resonance coupling parameters.

The values of the tensor polarization t_{20} are not taken as quantities to be fitted, but are instead obtained as a prediction. We thus intend to check which of the two discrepant sets of measurements[13,14] is favored by our analysis.

The theoretical curves for $d\sigma/d\Omega$ and iT_{11} calculated with the pure Faddeev amplitudes are represented by the cross-dashed lines in Figs. 2 and 3 for the RS case and in Figs. 4 and 5 for the Lyon case. For $d\sigma/d\Omega$ we see that the RS and Lyon results present similar structures, with the Lyon amplitudes giving better description of the data at 180 MeV; at 256 MeV both theoretical calculations are far from the data at middle and large angles. As for the values of iT_{11}, the RS amplitudes reproduce the data more closely than the Lyon amplitudes. The differences in the two background sets of amplitudes may lead us to somewhat different information about the ΔN interaction in the intermediate state.

We describe below a selection of results obtained from our numerical work. We present separately the results based on the RS and on the Lyon sets.

A. Influence of dibaryon resonances

1. RS background

The effects of the 4^+ resonance are negligible, even if only a separate fitting of the observables at 256 MeV is performed. This is in accordance to the conclusions of our previous analysis.[7] The 2^+ and 3^- contributions, however, lead to a noticeable improvement of the differential cross section at 180 and 256 MeV [see the three dot-dashed curves in Figs. 2(b) and (c)], the other observables remaining practically unaltered. For both 2^+ and 3^- resonances we obtain the best (but by no means good) fit for $F_J \approx 0°$ and $E_J \approx 90°$, i.e., dominant coupling to the $L=J$ orbital. The spin $S=2$ value is favored over $S=1$: with H_J left free we obtain $H_2 = -12°$, $H_3 = -24°$.

2. Lyon background

Here the contributions of the dibaryon resonances tend to improve the iT_{11} values at 180 and 256 MeV, with very small effect on this quantity at 142 MeV. However, at the same time the fits of the differential cross sections tend to become worse. In the joint fit of iT_{11} and $d\sigma/d\Omega$, practically the only gain occurs at 256 MeV, where the 2^+ resonance improves slightly $d\sigma/d\Omega$, and the 4^+ resonance improves iT_{11}. However the effects are unimportant, and are not represented in the figures.

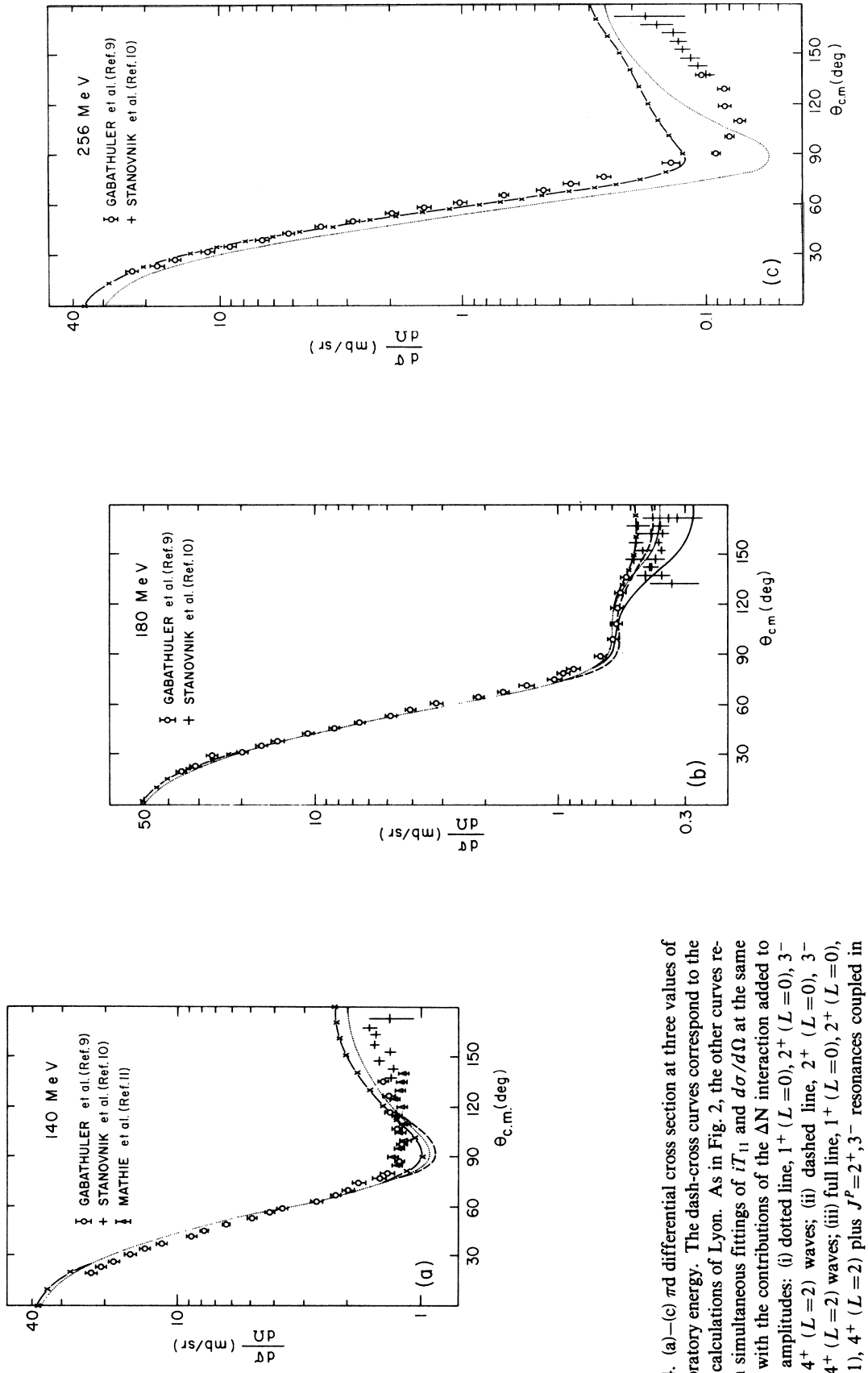

FIG. 4. (a)–(c) πd differential cross section at three values of pion laboratory energy. The dash-cross curves correspond to the Faddeev calculations of Lyon. As in Fig. 2, the other curves result from simultaneous fittings of iT_{11} and $d\sigma/d\Omega$ at the same energies, with the contributions of the ΔN interaction added to the Lyon amplitudes: (i) dotted line, 1^+ ($L=0$), 2^+ ($L=0$), 3^- ($L=1$), 4^+ ($L=2$) waves; (ii) dashed line, 2^+ ($L=0$), 3^- ($L=1$), 4^+ ($L=2$) waves; (iii) full line, 1^+ ($L=0$), 2^+ ($L=0$), 3^- ($L=1$), 4^+ ($L=2$) plus $J^P=2^+,3^-$ resonances coupled in $L=J$ orbitals (no sensible improvement is obtained by adding the 4^+ resonance). The full line is represented only in (b) because at 142 and 256 MeV the improvement obtained over the dotted curve is negligible. At 256 MeV, cases (ii) (dashed), (iii) (full), and (i) (dotted) are indistinguishable.

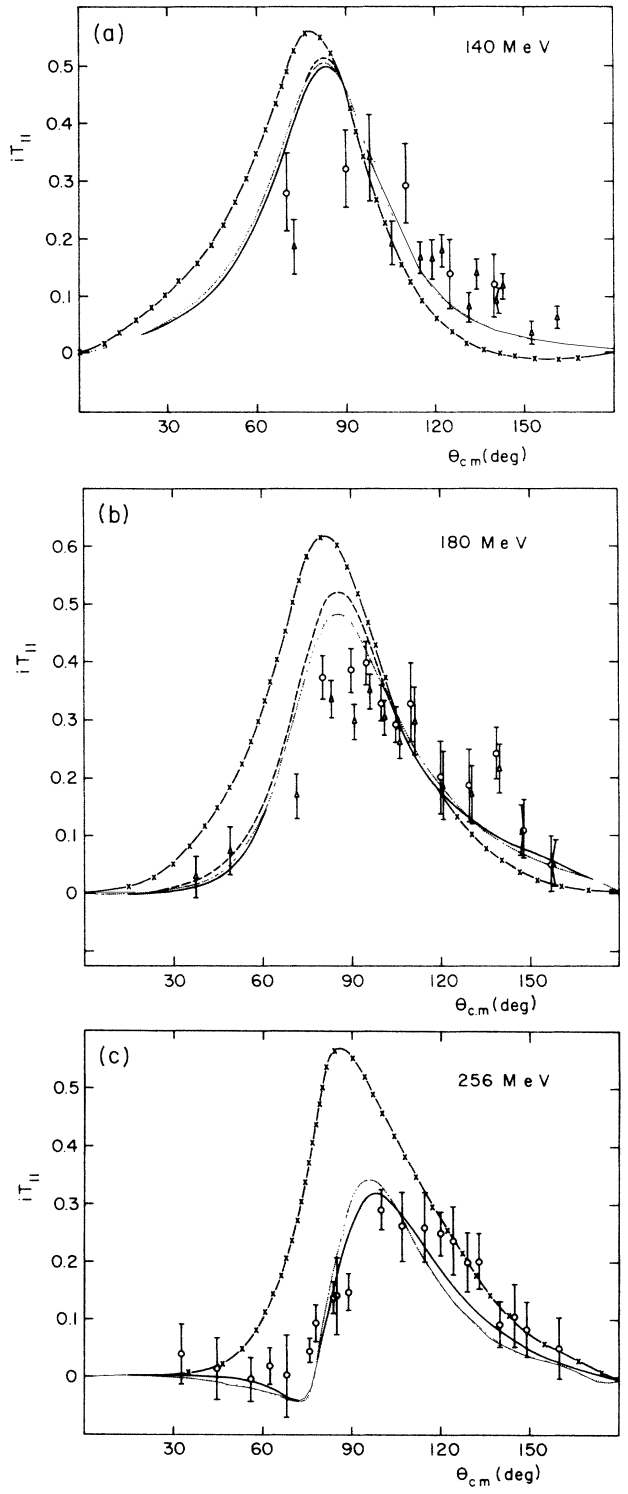

FIG. 5. (a)—(c) Vector analyzing power iT_{11} at three values of pion laboratory energy, evaluated with background of Lyon amplitudes plus contributions from the ΔN interaction. For meaning of curves see caption to Fig. 4. The experimental points are from Smith *et al.* (Ref. 12). In (a), case (ii) (dashed) almost coincides with (i) (dotted) and is represented only at angles near 80 degrees; for angles larger than 90 degrees, cases (i) and (ii) are indistinguishable. In (c), case (ii) (dashed) practically coincides with case (i) (dotted) and is not represented. The full line (iii) is not represented where it coincides with the dotted line.

TABLE III. ΔN interaction parameters (phase shifts) obtained from the fitting using the background of RS amplitudes. All absorption parameters $\eta_{J,L,S}$ result equal to one.

	J^P,L	$1^+,0$	$2^+,0$	$3^-,1$
T (MeV)	$\sqrt{s}$ (GeV)	δ (deg)	δ (deg)	δ (deg)
142	2.14	−60	46	68
180	2.18	−65	39	49
256	2.24	−5	18	13

B. Influence of unconstrained interaction in the low L partial waves

We have experimented with all states of Table I, using up to five waves simultaneously.

1. RS background

Our numerical analysis showed that in order to obtain a reasonable agreement with experiment the 2^+ ($L=0$) and 3^- ($L=1$) waves cannot be absent: 2^+ is essential to improve $d\sigma/d\Omega$ at 180 MeV, and 3^- for iT_{11} at all energies. The improvements are shown in Figs. 2(b) and 3(a)—(c) in dotted lines, and in Fig. 2(c) in dot-dashed lines. Inclusion of the 1^+ ($L=0$) contribution leads to further improvement of $d\sigma/d\Omega$ at 142 and 180 MeV.

The differential cross section at 256 MeV cannot be fitted even with such a large number of parameters. This shows how strongly limited are the effects of the free choice of parameters in the ΔN interaction.

The phases and resonance parameters obtained for the ΔN interaction with this fitting are shown in Tables III and IV. For all $L=J-2$ waves we obtain no absorption ($\eta\approx 1$) and no indication of resonance behavior of the phases. The resonances are more likely to couple to the $S=2$, ΔN state: when left free, H_J takes small values.

2. Lyon background

The general picture is similar to the RS case discussed above. Again the 2^+ ($L=0$) and the 3^- ($L=1$) contributions are the most effective ones, being responsible for almost all improvement that can be obtained. The 2^+ contribution is more important for iT_{11} at 142 MeV and for $d\sigma/d\Omega$ at 256 MeV, while the 3^- wave is more effective for iT_{11} at 180 and 256 MeV and for $d\sigma/d\Omega$ at 180 MeV.

The additional 4^+ ($L=2$) contribution (in addition to the 2^+ and 3^- waves) leads to further improvement in iT_{11} at 142 and 180 MeV. The results obtained with the joint contributions of these three waves are shown in

TABLE IV. Values obtained for the resonance parameters g_J (in GeV) and H_J (in degrees) in the case of RS amplitudes. For both resonances $E_J=\pi/2$ and $F_J=0$, which means that the $L=J$ orbitals are the most strongly coupled.

J^P	2^+	3^-
g_J (GeV)	2.4	2.8
H_J (deg)	6	−1

TABLE V. ΔN interaction parameters (phase shifts) obtained from the fitting using the background of Lyon amplitudes. All absorption parameters $\eta_{J,L,S}$ result equal to one.

J^P,L		$1^+,0$	$2^+,0$	$3^-,1$	$4^+,2$
T (MeV)	$\sqrt{s}$ (GeV)	δ (deg)	δ (deg)	δ (deg)	δ (deg)
142	2.14	−21	57	60	−82
180	2.18	−35	25	40	−94
256	2.24	4	44	110	−35

dashed lines in Figs. 4 and 5.

Including the 1^+ ($L=0$) wave as a fourth contribution leads to some improvement in both $d\sigma/d\Omega$ and iT_{11} at 142 and 180 MeV, but not at 256 MeV. The results are shown in dotted lines in Figs. 4 and 5.

Adding to this set of four unconstrained waves the contributions of the dibaryon resonance couplings in the $L=J$ and $L=J+2$ orbitals, the only remarkable effect is seen in the differential cross section at 180 MeV, mainly due to the contribution of the 3^- resonance. The fitting results are shown in solid lines, in the cases when they differ appreciably from the dotted lines. Concentrating on the $J=2$ and $J=3$ states, we have also tried the fittings with the two unconstrained waves in the presence of the resonance couplings. The results, which are not represented in the figures, are the same as when the 4^+ and 1^- waves are also present, i.e., only $d\sigma/d\Omega$ at 180 MeV is remarkably influenced by the resonance couplings in the $L=J, J+2$ orbitals.

The phases and resonance parameters are given in Tables V and VI. There is no absorption ($\eta=1$), and the 3^- ($L=1$) phase shift passes through 90° near the position of the 3^- resonance. We must observe that the rather strong values of the phases for the 4^+ ($L=2$) ΔN interaction, in spite of the comparatively small influence of this wave in the results of the fitting, is due to the rather low values of the vertex function $F_L(s)$ for $L=2$, as compared to the $L=0$ and $L=1$ ones.

C. Predictions for t_{20}^{lab}

The available experimental data for t_{20}^{lab} at the large angle $\theta=144°$ are shown in Fig. 6. At 142 MeV, two groups[13,14] have made measurements, with contradictory results, giving opposite signs for the value of t_{20}^{lab}. At 180 and 256 MeV, only one experiment has been made. The results of our analysis are shown in the same figure. At 142 MeV, the calculation with the Lyon amplitudes, with or without the ΔN interaction (full and open triangles, respectively), gives values around zero, which are closer to the experimental points of König *et al.*,[13] while the RS amplitudes plus the ΔN interaction (full square) reproduce the experimental point of Ungricht *et al.*[14] At 180 MeV, both sets of amplitudes plus the ΔN contributions give results in perfect agreement with the experimental point. At 256 MeV, no agreement is obtained with the data point, the ΔN interaction contributions taking the theoretical points upwards and away from the data. We recall that the differential cross section has also been impossible to fit with our ΔN contributions at this energy and angle. It is remarkable that at the same time iT_{11} is well reproduced, as can be seen in Figs. 3(b) and 5(c). It is clear that some ingredient is missing in the Faddeev calculation of the πd elastic amplitudes at 256 MeV.

TABLE VI. Values obtained for the resonance parameters g_J (in GeV) and H_J (in degrees) in the case of a background of Lyon amplitudes. For both resonances $F_J=0$, which means that the observables are insensitive to the resonance couplings to the highest $L=J+2$ orbitals.

J^P	2^+	3^-
g_J (GeV)	2.6	3.0
H_J (deg)	6	−19

IV. CONCLUSIONS

The presently available (e.g., RS and Lyon) Faddeev calculations of πd scattering do not include short-range ΔN interactions and show significant discrepancies with respect to experiments. This has given us motivation for

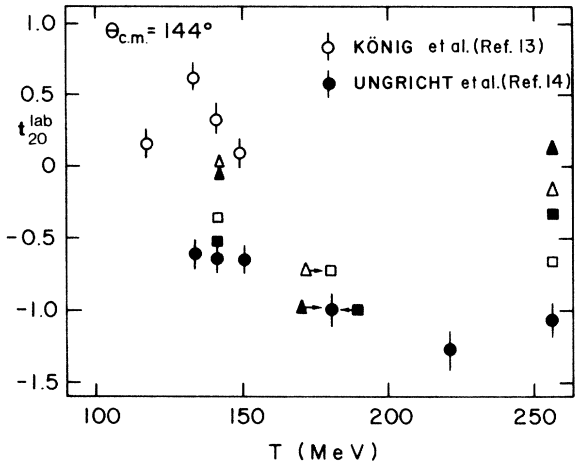

FIG. 6. Comparison of theoretical calculations of t_{20}^{lab} with the two existing sets of experimental results. Pure Faddeev calculations are shown in open squares (RS amplitudes) and open triangles (Lyon amplitudes). The predictions made from the best fittings of $d\sigma/d\Omega$ and iT_{11} are shown in full squares (background of RS amplitudes) and full triangles (background of Lyon amplitudes).

the present work, where we have introduced a unitary form for the ΔN interaction, which is incorporated into the πd scattering amplitude through the dynamical model of Fig. 1, whose evaluation is explained in detail in Refs. 6 and 7. The additional terms are small as compared with the unitarity limit, hence an addition of them to the Faddeev amplitudes does not violate the unitarity constraints essentially (see the Appendix for more details). In general they give only comparatively small corrections to the individual amplitudes, as can be seen from the fact that the differential cross sections in the forward hemisphere are hardly affected. On the other hand, we have shown that the quantities whose values result from cancellations among a large number of partial waves (such as $d\sigma/d\Omega$ at large angles) or from differences between helicity amplitudes (such as iT_{11}) are noticeably modified and thus may be used for an investigation of the ΔN interaction parameters.

The results of the attempt to improve the agreement between theory (Faddeev-type three-body calculations) and experiment in elastic πd scattering through the ΔN intermediate state interactions depend necessarily on the set of background amplitudes chosen.

For the RS background amplitudes we may get quite satisfactory agreement with experiment, except for the backward scattering cross section at 256 MeV. The main improvement stems from nonresonant interactions in the 2^+ ($L=0$) and 3^- ($L=1$) ΔN states. Additional waves and resonance contributions improve the agreement in detail, but not essentially. Especially, we find no indication for a 4^+ resonance. The latter result is in full agreement with our more general findings,[7] where we concluded that, independently of the background amplitudes, a 4^+ resonance with the couplings parameters of Ref. 8 cannot be accommodated in the conventional dynamical picture represented by Fig. 1. The predicted values for t_{20}^{lab} are in satisfactory agreement at 142 and 180 MeV, and in strong disagreement at 256 MeV, with respect to the experimental data of Ref. 14. Our results agree also qualitatively with those of Rinat,[15] who found that nonresonant ΔN interactions can improve the agreement with the experimental values of the vector analyzing power substantially.

In the case of the background of Lyon amplitudes the most remarkable improvements are obtained for $d\sigma/d\Omega$ at 180 MeV and for iT_{11} at 256 MeV. The experimental differential cross section at 142 MeV and the vector analyzing power at 142 and 180 MeV are not satisfactorily reproduced. As occurs with the RS case, the main improvements are due to the 2^+ ($L=0$) and 3^- ($L=1$) ΔN interactions. Additional waves contribute to details, with the 4^+ ($L=2$) and the 1^+ ($L=0$) coming first in order of importance. The resonance couplings in the $L=J$ and $L=J+2$ orbitals can hardly have their effects noticed, except for $d\sigma/d\Omega$ at 180 MeV, where the 3^- resonance has its influence seen. We must remark that perhaps the lowest orbital $L=J-2$ coupling of the 3^- resonance is responsible for the resonantlike behavior of the 3^- ($L=1$) phase, as shown in Table III.

In general, we can observe that for quantities in which the theoretical calculations present strong discrepancies with respect to the experimental data (or with respect to each other), the ΔN contribution can hardly lead to a satisfactory fitting. We must interpret that in such cases there are problems with the evaluation of the Faddeev amplitudes used for background. This is certainly the case with the differential cross section at 256 MeV.

We find that it is remarkable that the ΔN interaction in 2^+ ($L=0$) and 3^- ($L=1$) states play a fundamental role for the fitting results, in both cases of RS and Lyon amplitudes. We observe that these are the states in which there has been observed resonant behavior in the phases of proton-proton scattering. The corresponding values obtained for the ΔN phases shown in Tables II and III are quite compatible with each other at the energies of 142 and 180 MeV; of course no quantitative results for the ΔN parameters can be extracted at 256 MeV, due to the remaining strong discrepancies between the theoretical and experimental results at this energy. It is also interesting that our results for the ΔN phase shifts are compatible with those obtained for the 2^+ ($L=0$) ΔN state by Laget[16] in an analysis of pion photoproduction on deuterons, and are also compatible with the ΔN phases obtained[4] through the coupled channel K-matrix analysis of the NN phases in the $^1D_2$ state.

We must observe that our information referring to the 4^+ ($L=2$) state can only be considered as qualitative indications at the present, because the F_L vertex function is rather small for $L=2$ (as compared to the values of the vertex function for $L=0$), and the level of discrepancies and uncertainties in the background amplitudes and in other quantities are still rather large.

Our present analysis refers only to the elastic ΔN interaction represented in Fig. 1. The important ΔN→NN transition amplitudes can be studied through their contributions to the πd→NN process. We are now working in this direction.

This study stresses the importance of the effects of the ΔN interaction in πd physics, as it is already known to be the true of π-nuclear physics in general. It also stresses the need for a more complete and reliable description of the πd system as a three-body system, since the background of well determined amplitudes is an essential requirement for the investigation of additional dynamical effects.

This work has been partially supported by Deutscher Akademischer Austauschdient (DAAD) (Federal Republic of Germany) and by Financiadora de Estudos e Projetos (FINEP) and Conselho Nacional de Pesquisas (CNPq) (Brasil).

APPENDIX

In this appendix we explain the role of the unitarity constraints in our calculation. The dominant contribution to the s-channel unitarity relation of elastic πd scattering

$$i\langle \pi d \mid T^+ - T \mid \pi d \rangle = \sum \langle \pi d \mid T \mid z \rangle \langle z \mid T^+ \mid \pi d \rangle$$

is the intermediate NNπ channel. Therefore the old fashioned impulse approximation,[17] represented by the diagram of Fig. 7(a), not only gives a fairly good description of the process[18] but also satisfies the unitarity condition

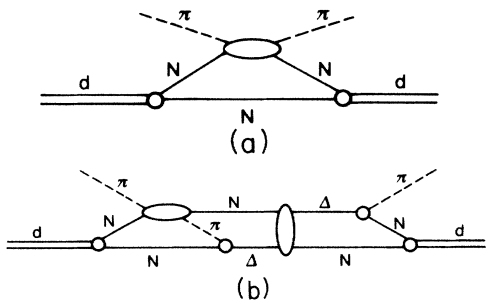

FIG. 7. (a) Skeleton diagram for the impulse approximation contribution. (b) A typical contribution missing in our approach, which should be included in a fully unitary treatment.

reasonably well. The impulse approximation calculation is improved by solving the Faddeev equations. This last procedure can be viewed as an inclusion of corrections to the simple graph in Fig. 7(a) which are required to guarantee unitarity.

However, the contribution of the diagram in Fig. 1, representing short range ΔN interactions in the intermediate state, has not been included in the Faddeev calculations, and it would be technically rather involved to do it. We have therefore just added the contribution of the graph in Fig. 1 to the Faddeev amplitudes. This approach does not take into account the influence of the short range ΔN interaction on the *corrections* to the impulse approximation, i.e., we have neglected contributions such as those represented in Fig. 7(b).

The contributions due to the ΔN interaction have been studied in Refs. 6 and 7. As can be read from Table II and from Eq. (27) of Ref. 7, the helicity amplitudes can at most reach about ten percent of the unitarity limit (taking the ΔN phases as 90 degrees). The corrections to the impulse approximation are of similar order of magnitude, i.e, the effects of the combined contributions, which are not taken into account but are present in the unitarity relation, can be estimated to be of only a few percent.

It should be emphasized again that the phase of the short range ΔN contribution is fixed completely by the diagram of Fig. 1. This has imposed severe restrictions on our fit.

[1]A. S. Rinat and Y. Starkand, Nucl. Phys. **A397**, 381 (1983); and private communication. We thank Dr. Rinat for the numerical table of amplitudes.

[2]N. Giraud, C. Fayard, and G. H. Lamot, Phys. Rev. C **21**, 1959 (1980); T. Mizutani *et al.*, Phys. Rev. C **24**, 2633 (1981); Phys. Lett. **107B**, 177 (1981). We thank the Lyon group for the numerical values of the amplitudes.

[3]B. Blankleider and I. R. Afnan, Phys. Rev. C **24**, 1572 (1981).

[4]B. J. Edwards and G. H. Thomas, Phys. Rev. D **22**, 2772 (1980); B. J. Edwards, *ibid.* **23**, 1978 (1981). For a study of the effects of the ΔN interaction in πd scattering, see A. Matsuyama and K. Yazaki, Nucl. Phys. **A364**, 477 (1981), and references therein.

[5]H. G. Dosch, S. C. B. Andrade, E. Ferreira, and G. Pérez, Phys. Rev. C **29**, 1549 (1984).

[6]H. G. Dosch and E. Ferreira, Phys. Rev. C **29**, 2254 (1984).

[7]H. G. Dosch and E. Ferreira, Phys. Rev. C **32**, 496 (1985).

[8]K. Kubodera *et al.*, J. Phys. G **6**, 171 (1980); M. P. Locher and M. E. Sainio, Phys. Lett. **121B**, 227 (1983); M. Akemoto *et al.*, Phys. Rev. Lett. **50**, 400 (1983); W. Jauch, A. König, and P. Kroll, Phys. Lett. **143B**, 509 (1924); E. Ferreira and G. Pérez, J. Phys. G **9**, 169 (1983).

[9]K. Gabathuler *et al.*, Nucl. Phys. **A350**, 253 (1980).

[10]A. Stanovnik *et al.*, Phys. Lett. **94B**, 323 (1980).

[11]E. L. Mathie *et al.*, Phys. Rev. C **28**, 2558 (1983).

[12]G. R. Smith *et al.*, Phys. Rev. C **29**, 2206 (1984).

[13]V. König *et al.*, J. Phys. G **9**, L211 (1983).

[14]E. Ungricht *et al.*, Phys. Rev. Lett. **52**, 333 (1984); Phys. Rev. C **31**, 934 (1985).

[15]A. S. Rinat, Phys. Lett. **126B**, 151 (1983).

[16]J. M. Laget, Proceedings of the 1984 Workshop on Electron and Photon Interactions at Medium Energies, Bad-Honef, Federal Republic of Germany, Report No. DPL-N/Saclay 2223, 1984.

[17]G. F. Chew, Phys. Rev. **80**, 196 (1950).

[18]E. Ferreira, L. Pinguelli Rosa, and Z. D. Thomé, Phys. Rev. C **16**, 2353 (1977).